



Article

# Genome Editing of Golden SNP-Carrying Lycopene Epsilon-Cyclase (*LcyE*) Gene Using the CRSPR-Cas9/HDR and Geminiviral Replicon System in Rice

Jong Hee Kim <sup>1</sup>, Jihyeon Yu <sup>2</sup>, Hee Kyoung Kim <sup>1</sup>, Jin Young Kim <sup>1</sup>, Me-Sun Kim <sup>3</sup>, Yong-Gu Cho <sup>3</sup>, Sangsu Bae <sup>4</sup>, Kwon Kyoo Kang <sup>1,5</sup> and Yu Jin Jung <sup>1,5,\*</sup>

<sup>1</sup> Division of Horticultural Biotechnology, School of Biotechnology, Hankyong National University, Anseong 17579, Korea

<sup>2</sup> Division of Life Sciences, Korea Polar Research Institute, Incheon 21990, Korea

<sup>3</sup> Department of Crop Science, Chungbuk National University, Cheongju 28644, Korea

<sup>4</sup> Department of Biomedical Sciences, Seoul National University College of Medicine, Seoul 03080, Korea

<sup>5</sup> Institute of Genetic Engineering, Hankyong National University, Anseong 17579, Korea

\* Correspondence: yuyu1216@hknu.ac.kr; Tel.: +82-31-670-5101



**Citation:** Kim, J.H.; Yu, J.; Kim, H.K.; Kim, J.Y.; Kim, M.-S.; Cho, Y.-G.; Bae, S.; Kang, K.K.; Jung, Y.J. Genome Editing of Golden SNP-Carrying Lycopene Epsilon-Cyclase (*LcyE*) Gene Using the CRSPR-Cas9/HDR and Geminiviral Replicon System in Rice. *Int. J. Mol. Sci.* **2022**, *23*, 10383. <https://doi.org/10.3390/ijms231810383>

Academic Editor: Kenji Miura

Received: 18 August 2022

Accepted: 4 September 2022

Published: 8 September 2022

**Publisher's Note:** MDPI stays neutral with regard to jurisdictional claims in published maps and institutional affiliations.



**Copyright:** © 2022 by the authors. Licensee MDPI, Basel, Switzerland. This article is an open access article distributed under the terms and conditions of the Creative Commons Attribution (CC BY) license (<https://creativecommons.org/licenses/by/4.0/>).

**Abstract:** Lycopene epsilon-cyclase (*LcyE*) is a key enzyme in the carotenoid biosynthetic pathway of higher plants. Using the CRSPR/Cas9 and the geminiviral replicon, we optimized a method for targeted mutagenesis and golden SNP replacement of the *LcyE* gene in rice. We have exploited the geminiviral replicon amplification as a means to provide a large amount of donor template for the repair of a CRISPR-Cas-induced DNA double-strand break (DSB) in the target gene via homology-directed repair (HDR). Mutagenesis experiments performed on the Donggin variety achieved precise modification of the *LcyE* loci with an efficiency of up to 90%. In HDR experiments, our target was the *LcyE* allele (*LcyE*-H523L) derived from anther culture containing a golden SNP replacement. The phenotype of the homologous recombination (HR) mutant obtained through the geminiviral replicon-based template delivery system was tangerine color, and the frequency was 1.32% of the transformed calli. In addition, the total carotenoid content of the *LcyEsg2*-HDR1 and *LcyEsg2*-HDR2 lines was 6.8–9.6 times higher than that of the wild-type (WT) calli, respectively. The reactive oxygen species content was lower in the *LcyEsg2*-HDR1 and *LcyEsg2*-HDR2 lines. These results indicate that efficient HDR can be achieved in the golden SNP replacement using a single and modular configuration applicable to different rice targets and other crops. This work demonstrates the potential to replace all genes with elite alleles within one generation and greatly expands our ability to improve agriculturally important traits.

**Keywords:** gene replacement; homology-directed repair (HDR); CRISPR-Cas9; geminiviral replicons; genome editing; *LcyE*; rice

## 1. Introduction

Targeted genome editing has become a powerful genetic tool for studying gene function and for introducing new functions or modifying the genome to correct defective genes. Therefore, it is becoming a very important tool in plant breeding compared to the random mutagenesis and recombination techniques that have been used previously to generate novel genetic variation. Accurate genome editing has been achieved through the use of targeted double-strand break (DSB) induction through the clustered regularly spaced short palindromic repeats (CRISPR) and CRISPR-associated protein 9 (Cas9) systems [1]. To date, many studies have demonstrated the potential of CRISPR-Cas9-mediated genome editing to induce specific indel mutations, gene targeting (GT), and controlled gene expression [2–10]. However, GT or gene replacement is possible but still not a routine method due to its low frequency. Various methods have been reported over the years to increase the frequency

of HDR between genomic targets and extrachromosomal homologous donors [11–14]. In plants, HDR or gene replacement required the coordination between the induction of DSBs from genomic targets and the existence of donor recovery templates in the cells. However, in the plant genome engineering field, the non-homologous end joining DNA repair pathway (NHEJ) mediated by the knockout method is still favored over the HDR method. The reason for this is that it is difficult to deliver a sufficient copy number of donor repair templates (DRT) in the cell for HDR, and the DRT stability in the cell is not guaranteed. It is quite challenging to deliver a DRT into a plant for the HDR-mediated repair of a DSB. Recently, Wang et al. [15] reported that they established a geminiviral replicon-based donor template delivery system to increase the frequency of gene knock-in in rice. Due to the high copy number and single-stranded DNA nature of the geminiviral genome, these genomes can be used as DNA template carriers for GT in plants. To date, successful gene targeting with the geminiviral replicon system required selection markers associated with the edited allele, indicating that targeting plant genes without the use of selection markers is still a challenge [16–18]. Therefore, GTs in plants, especially alleles without selectable markers, still need to be improved with many studies. Carotenoids are synthesized in plastids and accumulated as red, orange, and yellow pigments, among which  $\beta$ -carotene, lycopene, and lutein are industrially important components as powerful antioxidants [19]. The cyclization of lycopene ends catalyzed by lycopene  $\beta$ -cyclase and lycopene  $\epsilon$ -cyclase forms  $\beta$ -carotene or  $\alpha$ -carotene. Wakasa et al. [20] reported the characteristics of two callus lines showing orange and tangerine colors by repeatedly subculturing anther culture-derived mutant calli. Ishihara et al. [21] showed that the tangerine callus line is the *LcyE* gene (H523L), which carries a single nucleotide polymorphism responsible for His to Leu substitution at amino acid position 523, exhibiting a dramatically higher carotenoid content than WT calli. Here, we created HDR callus mutants (*LcyEsg2*-HDR1 and *LcyEsg2*-HDR2) with golden SNP-carrying *OsLcyE* genes using the CRSPR/Cas9 and the geminiviral replicon system. Our results showed that the *LcyEsg2*-HDR1 and *LcyEsg2*-HDR2 lines increased the content of total carotenoids and reduced ROS accumulation under salt stress conditions.

## 2. Results

### 2.1. Efficient Allelic Replacement by the Geminiviral Replicon for Targeted Modifications

To accurately replace an existing allele in the genome with an elite allele without a selection marker, we improved the HDR strategy in the following ways using the geminiviral replicon previously reported by Dahan-Meir et al. [22]. First, we mutated the protospacer adjacent motif (PAM) site in the core sequence of the DRT to prevent the Cas9/gRNA from cleaving the DRT when the HDR was successful. We also created a recognition site of *Bam*HI in the DRT as a marker to identify HDR events (Figure 1A,B and Supplementary Figure S1). According to our strategy, we constructed a Ti-plasmid vector that expresses both Cas9 and gRNAs, which generate DSBs at the targeted genomic sites and release a DRT from the plasmid (Figure 1C, Supplementary Table S1, and Figure S2). Therefore, these T-plasmid vectors contain all the components for replacement with *OsLcyE* (H523L) (Figure 1). The transformed calli were subcultured three times in 2N6 medium containing 6 mg/L of phosphinothricin. First, in order to determine whether the T-DNA region was introduced, the expected band was amplified in 95% of the results of the PCR analysis using the primer set NOS-barF/R (Figure 1D and Supplementary Figure S3). To confirm HDR events, a total of 387 transgenic calli were digested with *Bam*HI or subjected to deep sequencing. Notably, HDR occurred only in *LcyEsg2*; 1.32% (4/304) of the transgenic calli showed the intended precise HDR events (Figure 2D, Table 1). In addition, the majority (54.5%) of the mutation types were generated through NHEJ (Figure 2D and Table 1). Therefore, two of these four calli were selected and named *LcyEsg2*-HDR1 and *LcyEsg2*-HDR2, respectively, and were subcultured to analyze their characteristics (Figure 2A–C).

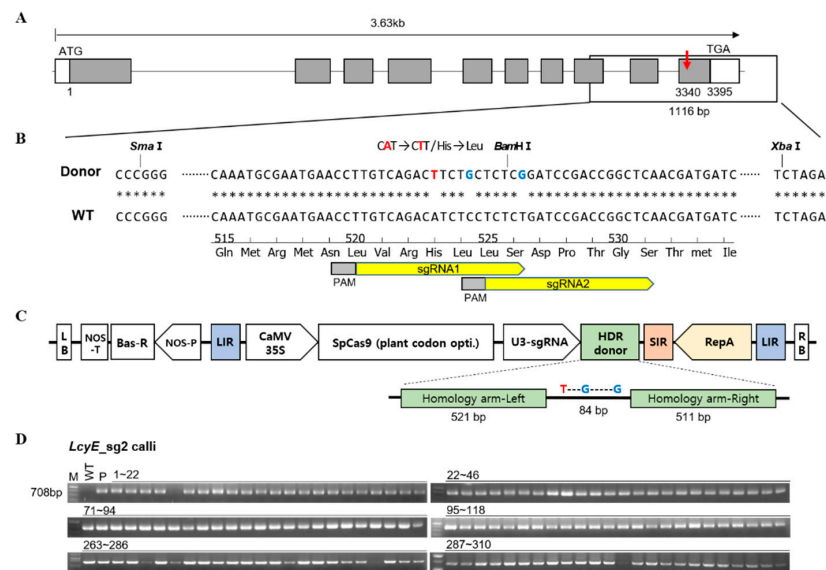


**Figure 1.** (A) Schematic representation of the *LcyE* gene and targeting sites. (B) The nucleotides highlighted in red correspond to intended modifications for SNP, and in blue are the silent mutations to avoid re-cutting and to generate cleaved amplified polymorphic sequence (CAPS) markers. Asterisks indicate identical nucleotides. The cutting sites of the two guide RNAs used in this study are indicated by two yellow arrows with PAM. (C) Schematic representation of the CRISPR/Cas9 vector and the homologous DNA donor template construction. (D) PCR analysis of the bar gene and the NOS terminator region (primer set NOS-bar F/R) in the rice callus introduced with the pGemBos::*LcyE* vector. M: 1 kb DNA ladder; WT: wild type; P: pGemBos::*LcyE* plasmid vector.

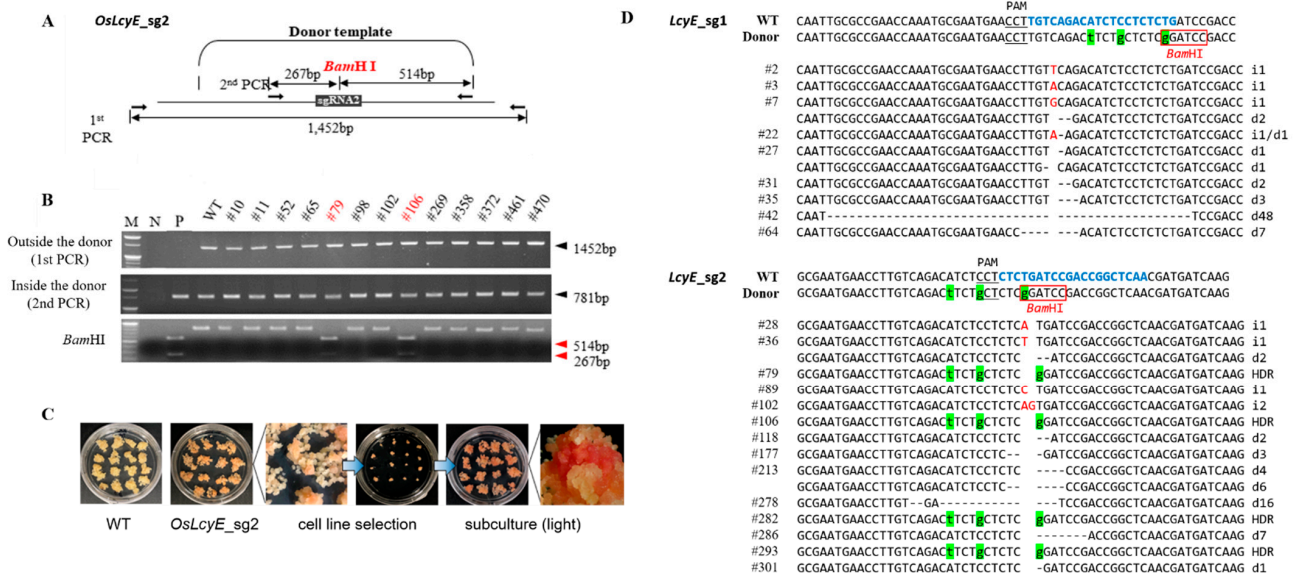


**Figure 2.** (A) Position of key SNP replacement of the *LcyE* targeted site (*Bam*HI restriction enzyme site was created inside the donor). (B) Screening by using PCR and restriction enzyme analysis. The second PCR products were digested with the *Bam*HI restriction enzyme. M: 1 kb DNA ladder; N: negative control; P: pGemBos::*LcyE\_sg2* plasmid vector; WT: wild type. (C) Phenotype of edited callus lines using the CRISPR-Cas9-based geminiviral replicon system in rice. (D) Mutation patterns of the target sequence region through deep sequencing. The target DNA sequence of *LcyE\_sg1* and *LcyE\_sg2* is shown in the WT with blue text at the top of the aligned sequences. The PAM sequences are underlined. Deletions are indicated as dashes; insertions are in red; and substitutes are in green highlighter. Indel sizes are shown on the right (i, insertion; d, deletion).

**Table 1.** HDR efficiency and mutation types for the *OsLcyE* gene using the CRISPR-Cas9-based geminiviral replicon system.

Targeted Region	No. of Examined Calli	DNA Repair Pathway	No. of Edited Calli (%)	Mutant Type	No. of Mutation
<i>LcyE</i> -sg1	83	NHEJ	48 (57.8%)	Homo	8
		HDR	0 (0%)	Bi-allelic	13
<i>LcyE</i> -sg2	304	NHEJ	169 (54.5%)	Hetero	27
		HDR	4 (1.32%)	-	-
		HDR	4 (1.32%)	Homo	24
				Bi-allelic	46
				Hetero	93
				Homo	4

## 2.2. Protein Model According to the Golden SNP Replacement of *OsLcyE*

In the *OsLcyE* gene, the golden SNP is replaced by HDR in exon 8 using the CRISPR-Cas9 system, resulting in an amino acid change from His to Leu. The *LcyEsg2*-HDR1 and *LcyEsg2*-HDR2 lines were investigated to find changes at the protein level that might explain the change of *LcyE* activity. By translating the mutant sequences and aligning them with the wild-type *LcyE*, we were able to identify key functional residues. We then used homology modeling to determine the effect of mutations on the structure and key functional residues of the enzyme (Figure 3). The *LcyEsg2*-HDR1 and *LcyEsg2*-HDR2 lines were changed from H to L at 523. Comparative models of the wild-type *LcyE* and mutant versions showed that the frame shift was caused by the replacement of the catalytic triad and the His<sup>523</sup> residue, which plays an important role in stabilizing the catalytic center (Figure 3). The *LcyE* structure of the wild type is linked by peptide chains of Leu<sup>183</sup>, Asp<sup>296</sup>, Tyr<sup>297</sup>, Ser<sup>306</sup>, His<sup>307</sup>, Pro<sup>308</sup>, and Asn<sup>407</sup>, whereas the *LcyE* structure of the HDR mutant lines is composed of Tyr<sup>182</sup>, Leu<sup>183</sup>, Gly<sup>185</sup>, Asn<sup>186</sup>, Lys<sup>187</sup>, Pro<sup>188</sup>, Ile<sup>189</sup>, Phe<sup>294</sup>, Asp<sup>296</sup>, Arg<sup>298</sup>, Phe<sup>301</sup>, Lys<sup>302</sup>, Ser<sup>306</sup>, and Thr<sup>324</sup>, which were converted into peptide chains (Figure 3). These mutant lines were replaced with golden SNP in the epsilon *Lyc* motif domain, resulting in slight changes in the enzymatic structure (Figure 3B). Thus, changes in the *LcyE* activity in the *LcyEsg2*-HDR1 and *LcyEsg2*-HDR2 lines reflect the de novo acquisition of a regulatory C-terminal domain that determines the substrate specificity of the catalytic center.

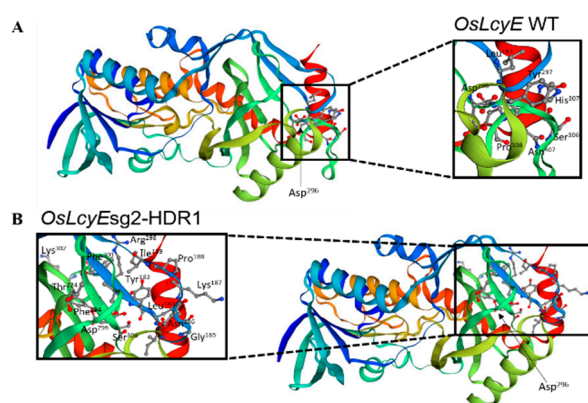


**Figure 3.** Structural comparison of the wild-type *OsLcyE* and the HDR-mutated version *OsLcyE*. (A) Wild-type *OsLcyE* showing the position of Asp<sup>296</sup>. The black box shows all of the key amino acids (Leu<sup>183</sup>, Asp<sup>296</sup>, Tyr<sup>297</sup>, Ser<sup>306</sup>, His<sup>307</sup>, Pro<sup>308</sup>, and Asn<sup>407</sup>). (B) Mutant *OsLcyE* showing the position of Asp<sup>296</sup>. The black box shows all of the key amino acids (Tyr<sup>182</sup>, Leu<sup>183</sup>, Gly<sup>185</sup>, Asn<sup>186</sup>, Lys<sup>187</sup>, Pro<sup>188</sup>, Ile<sup>189</sup>, Phe<sup>294</sup>, Asp<sup>296</sup>, Arg<sup>298</sup>, Phe<sup>301</sup>, Lys<sup>302</sup>, Ser<sup>306</sup>, and Thr<sup>324</sup>).

### 2.3. Carotenoid Analysis in the *LcyEsg2-HDR1* and *LcyEsg2-HDR2* Lines

The accumulated amounts of lycopene and  $\beta$ -carotene were determined by HPLC analysis using a standard curve obtained from an authentic compound. Unidentified carotenoid content eluted at 10.2, 30.2, 33.1, and 35.3 min was determined based on a standard curve for  $\beta$ -carotene. The *LcyEsg2-HDR1* and *LcyEsg2-HDR2* lines accumulated mainly lycopene with smaller amounts of carotene, such as lutein and  $\alpha$ -carotene. However, the WT line accumulated mainly  $\beta$ -carotene with another carotene (Table 2). The total amount of carotenoids in the *LcyEsg2-HDR1* and *LcyEsg2-HDR2* lines was approximately 15 times larger than that in WT calli.

**Table 2.** The content of carotenoids in *LcyEsg2-HDR1*, *LcyEsg2-HDR2* mutant, and WT calli.

Lines	Lycopene		Lutein		13Z- $\beta$ -Carotene		$\alpha$ -Carotene		$\beta$ -Carotene		9Z- $\beta$ -Carotene		Others		Total	
	Mean	SD	Mean	SD	Mean	SD	Mean	SD	Mean	SD	Mean	SD	Mean	SD	Mean	SD
WT	1.71	0.22	2.31	0.71	0.29	0.04	0.67	0.13	0.38	0.18	0.42	0.08	9.33	1.43	15.11	2.79
<i>LcyEsg2-HDR1</i>	205.1	36.0	2.87	0.10	0.23	0.01	1.08	0.41	0.09	0.01	0.44	0.02	21.11	1.21	230.92	37.76
<i>LcyEsg2-HDR2</i>	217.2	41.2	2.93	0.81	0.31	0.01	1.34	0.81	0.14	0.01	0.39	0.01	24.01	1.80	246.32	44.65

Data are expressed as means (the average value of content for dry weight) and SDs (the standard deviation value) of three independent experiments.

### 2.4. Reduced ROS Accumulation under Salt Stress Conditions

Given the high total carotenoid accumulation, we examined the effects of the *LcyEsg2-HDR1* and *LcyEsg2-HDR2* lines on the tolerance to oxidative stress induced by salt. Salt-induced oxidative stress in the calli was visualized by DAB staining, which turns to a dark brown when oxidized by  $H_2O_2$ . The *LcyEsg2-HDR1* and *LcyEsg2-HDR2* lines maintained a tangerine color, whereas the WT calli exhibited a dark brown color (Figure 4A). These results show that oxidative species and DAB reactants were reduced in response to NaCl stress in the *LcyEsg2-HDR1* and *LcyEsg2-HDR2* lines (Figure 4B).

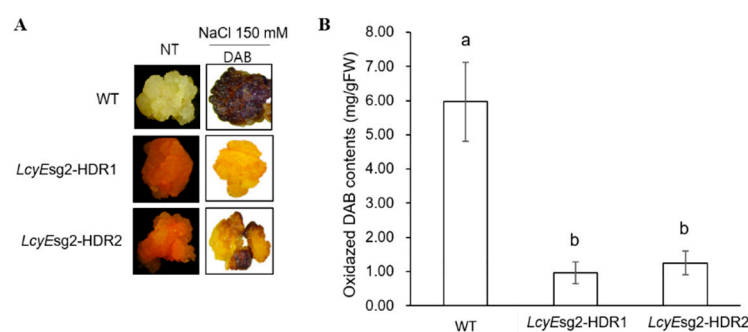


**Figure 4.** Salt-induced oxidative stress in the WT, *LcyEsg2-HDR1*, and *LcyEsg2-HDR2* lines was visualized by DAB staining in rice. (A) Visible damage in the WT, *LcyEsg2-HDR1*, and *LcyEsg2-HDR2* lines after stress treatment with 150 mM NaCl by DAB staining. NT: picture of the calli of each line before salt treatment. (B) Oxidized DAB contents in the WT, *LcyEsg2-HDR1*, and *LcyEsg2-HDR2* lines incubated at 150 mM NaCl. Bars indicate the standard error of the mean.

## 3. Discussion

To date, targeted mutations using the CRISPR-Cas9 system have already been shown in several plant species, including rice [23–25]. Among them, non-homologous end joining (NHEJ), which does not require a homologous template, is a pathway to repair double-strand breaks in DNA. However, since homology-directed repair requires homologous sequences to guide the repair, the substitution frequency is very low, so it is not yet routinely used. Therefore, many researchers have tried to increase the frequency of gene replacement using HDR [11–14,26]. For HDR to be possible in plants, NHEJs that induce DSBs in the

target genes must first be readily available. Second, so that the donor repair template (DRT) can be delivered very easily, the residence time of the intracellular donor, the donor size, and the culture conditions must be adjusted. Various strategies have been used to increase the availability of DRT to precisely modify plant genomes [15,17,27]. Despite such efforts, we believe that the reason HDR is not used routinely is because it is difficult to deliver a sufficient copy number of intracellular donor repair templates (DRT) for HDR, and intracellular DRT stability is not guaranteed. In this study, we achieved a homologous HDR frequency of 1.32% in rice calli using the CRISPR/Cas9 and geminiviral replicon systems (Table 1 and Figures 1 and 2D). Our HDR strategy is a system that allows for primary phenotypic selection by replacing the golden SNP (H523L) in *OsLcyE*, allowing for immediate color change of the calli (Figure 2A–C). In addition, when HDR occurs, base adjustments were made to the donor DNA so that it could be distinguished by the restriction enzyme *Bam*HI (Figures 1B and 2A,B). The gemini viruses used in this experiment are plant viruses with a single-stranded circular DNA genome (2.5–3.0 kb) and a broad host range, including monocot and dicot plants. Once infected, they are known to generate numerous replicons via rolling circle replication that can serve as repair templates during HDR [27,28]. To date, the frequency of successful HDR without antibiotic selection markers in donor DNA has been reported to be 0.07% in tomatoes [29] and 0.2–0.8% in rice [14,30,31]. In addition, the HDR success rate was very low in experiments using the herbicide tolerance gene for DRT in *Arabidopsis* [32]. Therefore, it is judged that the HDR system without antibiotics in plants is difficult to utilize for plant breeding unless the frequency of HDR is increased. In this respect, this study differs from previous reports in that there are no selectable markers in HDR, and it has shown promise to increase the success rate of HDR. Therefore, aspects of this study can be used for research to improve the frequency of HDR, such as the copy number of donors and the intracellular residence time for HDR. In particular, the *LcyEsg2*-HDR1 and *LcyEsg2*-HDR2 lines accumulated mainly lycopene with smaller amounts of carotene, such as lutein and  $\alpha$ -carotene (Table 2). The cause is thought to be due to differences in carotenoid biosynthesis activity or binding activity to the target protein according to the replacement of golden SNP in *OsLcyE*. According to our previous report, changes in carotenoid levels increased the salt stress tolerance [33]. Therefore, we investigated the effect of the *LcyEsg2*-HDR1 and *LcyEsg2*-HDR2 lines, which reduced ROS accumulation under salt stress conditions (Figure 4). Taken together, it is thought that the carotenoid biosynthesis intermediate obtained from the *LcyEsg2*-HDR1 and *LcyEsg2*-HDR2 lines produced higher amounts of antioxidants than the WT through cooperation with reactive oxygen species that reduced cell damage under salt stress. Although the HDR frequency is still much lower than NHEJ, the four independent precise HDR lines obtained are likely sufficient for the purpose of crop improvement. Therefore, our HDR system has broad applications in plant breeding, such as replacing disease susceptibility with disease resistance alleles in the same species that does not require back crossing or modifying key functional genes. In addition, this work demonstrates that the use of CRISPR/Cas9-mediated HDR for target allele replacement in rice without associative drag is feasible, effective, and significantly accelerates field-ready trait introgression in crop improvement.

#### 4. Materials and Methods

##### 4.1. Construction of Gene-Editing Vectors and *Agrobacterium*-Mediated Transformation

pGemBos, a plant binary vector for CRISPR-induced HDR, was modified from pTC217 (pTC217 was a gift from Daniel Voytas, Addgene: #70018) [26]. An AtU6 promoter and a GT donor were removed by a Cas9-RNP cut *in vitro*, and an sgRNA cassette drive by an OsU3 promoter and a multi-cloning site (MCS) for donor insertion were introduced using the Gibson assembly. A Basta resistance gene, phosphinothricin acetyltransferase, controlled by an NOS promoter and a terminator, was also introduced by an *Mlu*I cut and the Gibson assembly for the antibiotic selection in plants. Two CRISPR-Cas9 target sites in the *OsLcyE* sequences were selected using the Cas-designer (<http://www.rgenome.net/cas-designer/> accessed on 3 February 2020) [34] (Supplementary Figure S2). For CRISPR target sequences

regarding cloning, annealed pairs of oligonucleotides, synthesized by Bioneer Co., Ltd. (Dajeon, Korea), were cloned to pGemBos by a *Bsa*I cut. HDR donor sequences with golden SNP replacement mutations, and silence mutations at the target site were synthesized (Bioneer, Dajeon, Korea) and introduced to MCS by a *Sma*I cut. The constructs thus obtained were transformed into a rice embryogenic callus using *Agrobacterium tumefaciens* strain EHA105, as previously described [34]. The transformed callus was selected using 6 mg/L of phosphinothricin and confirmed by PCR analysis, as previously reported [6,7]. To verify the target site mutation, PCR amplicons were subjected to MiniSeq paired-end read sequencing (Illumina, San Diego, CA, USA) and analyzed using the Cas-Analyzer (<https://www.rgenome.net/cas-analyzer> accessed on 4 September 2020) [35]. All transgenic callus lines performed several subcultures and were maintained in 2N6 medium [6], described previously (Figure 2C).

#### 4.2. Total DNA Extraction and Mutation Detection

Total DNA extraction was performed by crushing 0.5 g of callus under liquid nitrogen with an electric drill in a 1.5 mL Eppendorf tube. A volume of 700  $\mu$ L of extraction buffer (0.8 M NaCl; 0.15 M sorbitol; 0.12 M Tris-HCl, pH 7.5; 22 mM EDTA; 0.8% CTAB; and 0.8% sodium lauroyl sarcosinate) was added to each tube and incubated for 20 min at 65 °C. A volume of 800  $\mu$ L of chloroform-isoamyl alcohol (24:1) was added to each tube and was centrifuged at 13,000 rpm for 5 min. This step was repeated twice. A volume of 1.4 mL of storage buffer (80% EtOH and 0.2 M sodium acetate) was added to the supernatant in a new 2 mL Eppendorf tube. DNA precipitation was performed by centrifugation at 13,000 rpm for 20 min at 4 °C. The pellet was re-suspended in 50  $\mu$ L of H<sub>2</sub>O. The extracted genomic DNA was then used as a template to amplify the relevant fragments from each of the target genes by using primers (Supplementary Table S2) flanking the target sites. The standard PCR conditions were as follows: 94 °C for 3 min; 94 °C for 30 s; 56 °C for 30 s; 72 °C for 30 s for 35 cycles; and 72 °C for 10 min. The PCR products were directly sequenced by NGS technology using internal sequencing primers (Supplementary Table S2) to identify mutations. The mutation rate of each target is calculated as a ratio, which is the number of transgenic calli edited in each target to the total number of transgenic calli obtained.

#### 4.3. Phenotypic Observations of the Golden SNP Replacement *LcyE* Mutant Calli

The phenotype of the HDR mutant calli substituted with H523L in the *OsLcyE* gene was confirmed by light microscopy in the second subculture after transformation and was photographed.

#### 4.4. Homology Modeling and Protein Structure Analysis

The *LcyE* sequence was translated, and the mature *OsLcyE* polypeptide (523 amino acids) was aligned with the mutant version from the *LcyEsg2*-HDR1 and *LcyEsg2*-HDR2 lines using the Unipro UGENE alignment platforms Kalign, MUSCLE, and ClustalW. Homology modeling was performed using Phyre2. The model of the mutant protein was overlaid on the wild-type version using DS Visualizer.

#### 4.5. Extraction of Pigments and Measurement of Absorption Spectra

After 28 days of subculture, the callus (0.1 g) was homogenized by crushing 0.5 g of the callus under liquid nitrogen. Acetone (1 mL) was added to the homogenate and mixed well. The supernatant after centrifugation at 13,000  $\times$ g rpm for 5 min at 4 °C was collected. This procedure was repeated, and the second supernatant was combined with the first supernatant, dried, and dissolved in 500  $\mu$ L acetone. This solution was diluted with acetone, and the absorption spectrum was measured using a spectrophotometer Ultrospec 3000 (Pharmacia Biotech, Seoul, Korea).

#### 4.6. Analysis of Carotenoid Contents

Carotenoids were extracted from callus tissues using a 0.01% solution of butylated hydroxytoluene in acetone and analyzed using an Agilent 1100 HPLC system (Hewlett Packard, Palo Alto, CA, USA) according to the method described by ref. [36].

#### 4.7. H<sub>2</sub>O<sub>2</sub> Assays

To measure cellular levels of H<sub>2</sub>O<sub>2</sub>, each callus was incubated in a 1 mg mL<sup>-1</sup> solution of 3,3-diaminobenzidine (DAB)-HCl (pH 3.8) for 5 h at 25 °C under light conditions according to the methods of [37]. For H<sub>2</sub>O<sub>2</sub> assays, the DAB solution was measured as the absorbance at 460 nm. Oxidized DAB concentrations were calculated from the standard curve of DAB.

#### 4.8. Statistical Analysis

All experiments included at least three independent technical and biological replicates, and data are presented as means ± standard error of the mean (SEM). All data analyses and processing were performed using Microsoft Excel 2019 (Microsoft Corporation, Anseong, Korea) and RStudio. Data for ROS experiments under salt stress conditions for the WT, *LcyEsg2*-HDR1, and *LcyEsg2*-HDR2 lines were compared using one-way ANOVA and Tukey's HSD. An analysis of variance was performed to look at the variation between groups and obtained the least significant difference at  $p < 0.05$ .

**Supplementary Materials:** The following supporting information can be downloaded at: <https://www.mdpi.com/article/10.3390/ijms231810383/s1>.

**Author Contributions:** Conceptualization, J.Y., S.B. and Y.J.J.; methodology, H.K.K., M.-S.K., J.Y. and S.B.; formal analysis, J.H.K., H.K.K. and J.Y.K.; writing—original draft preparation, J.H.K. and Y.J.J.; review and editing, J.Y., Y.-G.C. and K.K.K.; supervision, Y.J.J. All authors have read and agreed to the published version of the manuscript.

**Funding:** This work was supported by a grant from the New Breeding Technologies Development Program (Project No. PJ01686701). Rural Development Administration and basic science research program through the National Research Foundation of Korea (NRF) funded by the ministry education (2021R1I1A4A01057295) Republic of Korea.

**Institutional Review Board Statement:** Not applicable.

**Informed Consent Statement:** Not applicable.

**Data Availability Statement:** Not applicable.

**Conflicts of Interest:** The authors have no conflict of interest relevant to this study to disclose.

## References

1. Shan, Q.; Wang, Y.; Li, J.; Zhang, Y.; Chen, K.; Liang, Z.; Zhang, K.; Liu, J.; Xi, J.J.; Qiu, J.-L.; et al. Targeted genome modification of crop plants using a CRISPR-Cas system. *Nat. Biotechnol.* **2013**, *31*, 686–688. [CrossRef] [PubMed]
2. Ma, X.L.; Zhang, Q.Y.; Zhu, Q.L.; Liu, W.; Chen, Y.; Qiu, R.; Wang, B.; Yang, Z.F.; Li, H.; Lin, Y.R.; et al. A robust CRISPR/Cas9 system for convenient, high-efficiency multiplex genome editing in monocot and dicot plants. *Mol. Plant* **2015**, *8*, 1274–1284. [CrossRef] [PubMed]
3. Xie, W.; Lv, X.; Ye, L.; Zhou, P.; Yu, H. Construction of lycopene-overproducing *Saccharomyces cerevisiae* by combining directed evolution and metabolic engineering. *Metab. Eng.* **2015**, *30*, 69–78. [CrossRef] [PubMed]
4. Gao, X.; Chen, J.; Dai, X.; Zhang, D.; Zhao, Y. An effective strategy for reliably isolating heritable and Cas9-free *Arabidopsis* mutants generated by CRISPR/Cas9-mediated genome editing. *Plant Physiol.* **2016**, *171*, 1794–1800. [CrossRef] [PubMed]
5. Jung, Y.J.; Lee, G.J.; Bae, S.; Kang, K.K. Reduced ethylene production in tomato fruits upon CRISPR/Cas9-mediated *leMADS-RIN* mutagenesis. *Hortic. Sci. Technol.* **2018**, *36*, 396–405.
6. Jung, Y.J.; Lee, H.J.; Bae, S.; Kim, J.H.; Kim, D.H.; Kim, H.K.; Nam, K.H.; Nogoy, F.M.; Cho, Y.-G.; Kang, K.K. Acquisition of seed dormancy breaking in rice (*Oryza sativa* L.) via CRISPR/Cas9-targeted mutagenesis of *OsVP1* gene. *Plant Biotechnol. Rep.* **2019**, *13*, 511–520. [CrossRef]

7. Jung, Y.J.; Kim, J.H.; Lee, H.J.; Kim, D.H.; Yu, J.; Bae, S.; Cho, Y.-G.; Kang, K.K. Generation and transcriptome profiling of Slr1-d7 and Slr1-d8 mutant lines with a new semi-dominant dwarf allele of SLR1 using the CRISPR/Cas9 system in rice. *Int. J. Mol. Sci.* **2020**, *21*, 5492. [[CrossRef](#)]
8. Barrangou, R.; Doudna, J.A. Applications of CRISPR technologies in research and beyond. *Nat. Biotechnol.* **2016**, *34*, 933–941. [[CrossRef](#)]
9. Schaeffer, S.M.; Nakata, P.A. The expanding footprint of CRISPR/Cas9 in the plant sciences. *Plant Cell Rep.* **2016**, *35*, 1451–1468. [[CrossRef](#)]
10. Pacher, M.; Puchta, H. From classical mutagenesis to nuclease-based breeding—directing natural DNA repair for a natural end-product. *Plant J.* **2017**, *90*, 819–833. [[CrossRef](#)]
11. Shaked, H.; Melamed-Bessudo, C.; Levy, A.A. High-frequency gene targeting in Arabidopsis plants expressing the yeast RAD54 gene. *Proc. Natl. Acad. Sci. USA* **2005**, *102*, 12265–12269. [[CrossRef](#)] [[PubMed](#)]
12. Even-Faitelson, L.; Samach, A.; Melamed-Bessudo, C.; Avivi-Ragolsky, N.; Levy, A.A. Localized egg-cell expression of effector proteins for targeted modification of the *Arabidopsis* genome. *Plant J.* **2011**, *68*, 929–937. [[CrossRef](#)] [[PubMed](#)]
13. Kwon, Y.-I.; Abe, K.; Osakabe, K.; Endo, M.; Nishizawa-Yokoi, A.; Saika, H.; Shimada, H.; Toki, S. Overexpression of OsRecQ14 and/or OsExo1 enhances DSB-induced homologous recombination in rice. *Plant Cell Physiol.* **2012**, *53*, 2142–2152. [[CrossRef](#)] [[PubMed](#)]
14. Li, T.; Liu, B.; Chen, C.Y.; Yang, B. TALEN-mediated homologous recombination produces site-directed DNA base change and herbicide-resistant rice. *J. Genet. Genom.* **2016**, *43*, 297–305. [[CrossRef](#)]
15. Wang, M.; Lu, Y.; Botella, J.R.; Mao, Y.; Hua, K.; Zhu, J.K. Gene targeting by homology-directed repair in rice using a geminivirus-based CRISPR/Cas9 system. *Mol. Plant* **2017**, *10*, 1007–1010. [[CrossRef](#)]
16. Butler, N.M.; Baltés, N.J.; Voytas, D.F.; Douches, D.S. Geminivirus-mediated genome editing in potato (*Solanum tuberosum* L.) using sequence-specific nucleases. *Front. Plant Sci.* **2016**, *7*, 1045. [[CrossRef](#)]
17. Gil-Humanes, J.; Wang, Y.; Liang, Z.; Shan, Q.; Ozuna, C.V.; Sánchez-León, S.; Baltés, N.J.; Starker, C.; Barro, F.; Gao, C.; et al. High-efficiency gene targeting in hexaploid wheat using DNA replicons and CRISPR/Cas9. *Plant J.* **2017**, *89*, 1251–1262. [[CrossRef](#)]
18. Hummel, A.W.; Chauhan, R.D.; Cermak, T.; Mutka, A.M.; Vijayaraghavan, A.; Boyher, A.; Starker, C.G.; Bart, R.; Voytas, D.F.; Taylor, N.J. Allele exchange at the EPSPS locus confers glyphosate tolerance in cassava. *Plant Biotechnol. J.* **2018**, *16*, 1275–1282. [[CrossRef](#)]
19. Song, W.; Wei, F.; Gao, S.; Dong, C.; Hao, J.; Jin, L.; Li, F.; Wei, P.; Guo, J.; Wang, R. Functional characterization and comparison of lycopene epsilon-cyclase genes in *Nicotiana tabacum*. *BMC Plant Biol.* **2022**, *22*, 252. [[CrossRef](#)]
20. Wakasa, K.; Kobayashi, M.; Kamada, H. Colony formation from protoplasts of nitrate reductase-deficient rice cell lines. *J. Plant Physiol.* **1984**, *117*, 223–231. [[CrossRef](#)]
21. Ishihara, A.; Ohishi, K.; Yamada, T.; Shibata-Hatta, M.; Arai-Kichise, Y.; Watanabe, S.; Yoshikawa, H.; Wakasa, K. Biochemical and molecular characterization of orange-and tangerine-colored rice calli. *Plant Biotechnol.* **2015**, *32*, 193–203. [[CrossRef](#)]
22. Dahan-Meir, T.; Filler-Hayut, S.; Melamed-Bessudo, C.; Bocobza, S.; Czosnek, H.; Aharoni, A.; Levy, A.A. Efficient in planta gene targeting in tomato using geminiviral replicons and the CRISPR/Cas9 system. *Plant J.* **2018**, *95*, 5–16. [[CrossRef](#)] [[PubMed](#)]
23. Brooks, C.; Nekrasov, V.; Lippman, Z.B.; Van Eck, J. Efficient gene editing in tomato in the first generation using the clustered regularly interspaced short palindromic repeats/CRISPR-associated9 system. *Plant Physiol.* **2014**, *166*, 1292–1297. [[CrossRef](#)]
24. Pan, C.; Ye, L.; Qin, L.; Liu, X.; He, Y.; Wang, J.; Chen, L.; Lu, G. CRISPR/Cas9-mediated efficient and heritable targeted mutagenesis in tomato plants in the first and later generations. *Sci. Rep.* **2016**, *6*, 24765. [[CrossRef](#)]
25. Filler Hayut, S.; Melamed Bessudo, C.; Levy, A.A. Targeted recombination between homologous chromosomes for precise breeding in tomato. *Nat. Commun.* **2017**, *8*, 15605. [[CrossRef](#)]
26. Čermák, T.; Baltés, N.J.; Čegan, R.; Zhang, Y.; Voytas, D.F. High-frequency, precise modification of the tomato genome. *Genome Biol.* **2015**, *16*, 232. [[CrossRef](#)]
27. Baltés, N.J.; Gil-Humanes, J.; Cermak, T.; Atkins, P.A.; Voytas, D.F. DNA replicons for plant genome engineering. *Plant Cell* **2014**, *26*, 151–163. [[CrossRef](#)] [[PubMed](#)]
28. Hanley-Bowdoin, L.; Bejarano, E.R.; Robertson, D.; Mansoor, S. Geminiviruses: Masters at redirecting and reprogramming plant processes. *Nat. Rev. Microbiol.* **2013**, *11*, 777–788. [[CrossRef](#)] [[PubMed](#)]
29. Yu, Q.-H.; Wang, B.; Li, N.; Tang, Y.; Yang, S.; Yang, T.; Xu, J.; Guo, C.; Yan, P.; Wang, Q.; et al. CRISPR/Cas9-induced targeted mutagenesis and gene replacement to generate long-shelf life tomato lines. *Sci. Rep.* **2017**, *7*, 11874. [[CrossRef](#)]
30. Begemann, M.B.; Gray, B.N.; January, E.; Gordon, G.C.; He, Y.; Liu, H.; Wu, X.; Brutnell, T.P.; Mockler, T.C.; Oufattole, M. Precise insertion and guided editing of higher plant genomes using Cpf1 CRISPR nucleases. *Sci. Rep.* **2017**, *7*, 11606. [[CrossRef](#)]
31. Li, G.; Zhang, X.; Zhong, C.; Mo, J.; Quan, R.; Yang, J.; Liu, D.; Li, Z.; Yang, H.; Wu, Z. Small molecules enhance CRISPR/Cas9-mediated homology-directed genome editing in primary cells. *Sci. Rep.* **2017**, *7*, 8943. [[CrossRef](#)] [[PubMed](#)]
32. De Pater, S.; Klemann, B.J.; Hooymaas, P.J. True gene-targeting events by CRISPR/Cas-induced DSB repair of the PPO locus with an ectopically integrated repair template. *Sci. Rep.* **2018**, *8*, 3338. [[CrossRef](#)] [[PubMed](#)]
33. Ben Abdallah, S.; Aung, B.; Amyot, L.; Lalin, I.; Lachâal, M.; Karray-Bouroufi, N.; Hannoufa, A. Salt stress (NaCl) affects plant growth and branch pathways of carotenoid and flavonoid biosyntheses in *Solanum nigrum*. *Acta Physiol. Plant.* **2016**, *38*, 72. [[CrossRef](#)]

34. Park, J.; Bae, S.; Kim, J.S. Cas-Designer: A web-based tool for choice of CRISPR-Cas9 target sites. *Bioinformatics* **2015**, *31*, 4014–4016. [[CrossRef](#)]
35. Park, J.; Lim, K.; Kim, J.S.; Bae, S. Cas-analyzer: An online tool for assessing genome editing results using NGS data. *Bioinformatics* **2017**, *33*, 286–288. [[CrossRef](#)] [[PubMed](#)]
36. Lim, C.J.; Kim, H.Y.; Lee, C.H.; Kim, Y.U.; Back, K.W.; Bae, J.M.; Ahn, M.J. Variation in carotenoid composition in carrots during storage and cooking. *PNF* **2009**, *14*, 240–245. [[CrossRef](#)]
37. Kim, H.S.; Ji, C.Y.; Lee, C.J.; Kim, S.E.; Park, S.C.; Kwak, S.S. Orange: A target gene for regulating carotenoid homeostasis and increasing plant tolerance to environmental stress in marginal lands. *J. Exp. Bot.* **2018**, *69*, 3393–3400. [[CrossRef](#)]